Bending and buckling of rolled-up SiGe/Si microtubes using nanorobotic manipulation

Li Zhang, Lixin Dong, and Bradley J. Nelson[a)]
Institute of Robotics and Intelligent Systems, ETH Zurich, CH-8092 Zurich, Switzerland

(Received 26 March 2008; accepted 29 May 2008; published online 16 June 2008)

Mechanical properties of individual rolled-up SiGe/Si microtubes are investigated experimentally using nanorobotic manipulation. By applying bending loads, individual SiGe/Si microtubes demonstrate various deformation modes with increasing bending angle. Remarkably, the tested microtubes resist fracture even when bent back onto themselves (180° bending angle). Axial compression tests of microtubes with different turns are also performed. Among those tubes, 1.6-turn rolled-up SiGe/Si microtubes show typical Euler buckling behavior when the load is larger than a critical load, which can be estimated by the Euler formula for columns. © *2008 American Institute of Physics*. [DOI: 10.1063/1.2947590]

Si based micro-/nanotubes can be fabricated in a highly controllable fashion by employing the self-scrolling technique, which is based on strain relief between SiGe/Si bilayers or a pure Si layer with strain gradient after detachment from a Si substrate.[1–3] These tightly wound tubes have wall thicknesses in the nanometer range, high aspect ratios, and smooth surfaces. Their highly controllable fabrication with a variety of materials including semiconductors, metals, and insulators indicates a variety of potential applications in micro-/nanoelectromechanical systems[2] (MEMS/NEMS) Si based optoelectronics[4] and microfluidic devices.[5] It is obviously important to understand microtube material properties, however, little has been reported, although the fabrication technique is well developed. In this report, nanorobotic manipulation[6] is applied to investigate the mechanical properties of individual SiGe/Si microtubes.

Details on the fabrication of freestanding SiGe/Si microtubes have been described elsewhere.[7,8] The mesa pattern[7] used to fabricate freestanding microtubes is shown in Fig. 1(a), in which the ribbon width w is varied for the fabrication of tubes with different turns. Figures 1(b) and 1(c) show field emission scanning electron microscopy (FESEM) micrographs of an array of SiGe/Si microtubes and a single microtube, all with one fixed end, respectively. The initial planar thin films consist of an 11 nm thick SiGe layer with 40% Ge in the SiGe layer and an 8 nm Si layer on top.

For bending and buckling tests, the same manipulation technique is employed as previously reported.[9] To investigate the instability of microtubes by bending tests, the manipulator probe bends the tube with deflection angles between 0° and 180° to the substrate plane. To investigate the mechanical instability of microtubes under axial compressive loads, the individual SiGe/Si tube is manipulated using a sticky probe which is prepared by dipping the tip into a SEM compatible conductive tape. To cut individual freestanding SiGe/Si microtubes from the substrate by the sticky probe, a shear force is applied at the fixed end of the tube by lateral pushing of the sticky probe [see inset of Fig. 2(a)]. Then the microtube is mounted on the backside of an atomic force microscope (AFM) cantilever and rotated so that its axis is perpendicular to the AFM cantilever. The manipulation demonstrates that the boundary condition of the sticky probe and the microtube is "hinged," i.e., resembling a ball joint. Manipulation steps are demonstrated in Fig. 2. At the other end of the microtube, the boundary condition between an AFM cantilever and a microtube depends on the backside of the AFM cantilever. When an AFM cantilever has a smooth backside, the boundary condition can be considered free in the plane. Whereas for an AFM cantilever with a pyramid hole at the backside [see inset of Fig. 2(b)], the boundary condition becomes fixed. The fixed boundary condition is preferable. This makes it possible to adjust the angle between a tube and the manipulator probe to 90°, and the microtube will not readily slide during loading. By pushing the sticky probe along the tube axis, the microtube is subjected to an axial compressive stress and deflects the AFM cantilever. This deflection gives the compressive force applied to the longitudinal axes of the tube, from which the load and the stress on the microtube can be obtained.

The prepatterned SiGe/Si bilayer was scrolled into freestanding tubes with a diameter d of approximately 1.25 μm [see Fig. 1(c)], very close to the intended diameter.[10] Since the bilayer starts coiling from the both long sides of the stripe simultaneously, i.e., [100] and [−100], the width of the

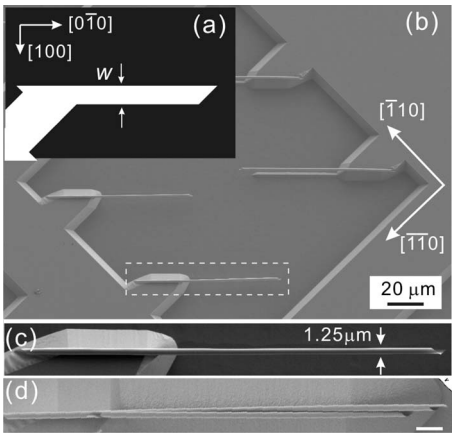

FIG. 1. (a) The initial mesa pattern used to fabricate freestanding SiGe/Si microtubes. The main scrolling directions of the bilayer are [100] and [−100]. (b) FESEM image of an array of SiGe/Si microtubes. The regions in the white dashed lines are magnified in (c). (d) FESEM image of a twin tube, the scale bar is 5 μm.

[a)]Electronic mail:bnelson@ethz.ch.

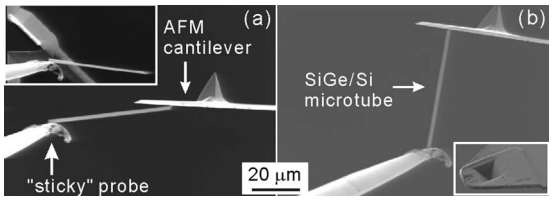

FIG. 2. Nanorobotic manipulation of a freestanding SiGe/Si microtube. (a) Placing a microtube on the backside of an AFM cantilever. Inset: Cutting of a microtube from the Si substrate. (b) Rotating a microtube on an AFM cantilever. Inset: AFM cantilever with a hole on its backside.

stripe w should be confined. According to our results, when the width of the stripe w is not larger than 1.6 times of the tube circumference, i.e., 1.6πd, a single freestanding tube can be achieved as shown in Fig. 1(c); whereas $w > 1.6\pi d$, "twin tubes" will be formed as shown in Fig. 1(d). The as-fabricated SiGe/Si microtubes are straight and have a uniform size from their free end to the fixed end. Microtubes with a freestanding length greater than 50 μm were employed for bending tests. The results from 1.6-turn tubes show that various deformation modes were observed depending on the bending angle. Under small deflection, i.e., not more than 10°, the horizontal diameter (d_h) of the whole freestanding part of the tube decreases as the cross section of tube becomes oval, demonstrating the Brazier effect,[11] in which the horizontal diameter reduces to approximately 15% with a 10° bending angle. By increasing the bending angle to 27.6°, the horizontal diameter decreased significantly in a local regime [see inset of Fig. 3(a)] due to local buckling of the tube.[11] The dependence of the horizontal diameter (d_h) on the tube axis (x) indicates that both local buckling and Brazier effects exist,[12] as shown in Fig. 3(c). If the microtube undergoes a larger bending angle, e.g., 95.5° as shown in Fig. 3(a), local buckling dominates the deformation of the tube, whereas the uniform Brazier effect disappears. In Fig. 3(c) the value of d_h is larger that of d, and is mainly attributed to the twisting of the tube in the buckled regime. If we release the bending force, the microtube recovers to its original shape and diameter as shown in Fig. 3(b). Interestingly, both 1.2- and 1.6-turn microtubes recover to their original

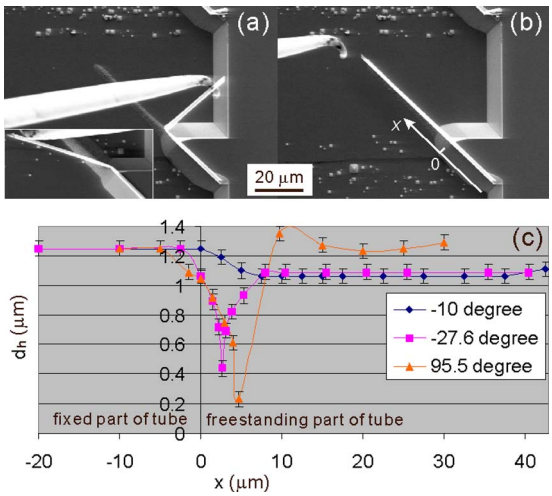

FIG. 3. (Color online) Bending tests of freestanding SiGe/Si microtubes. (a) A SiGe/Si microtube is buckled locally with a bending angle of 95.5° and −27.6° by the manipulator probe. (b) The tube recovers to its original shape after the probe is removed. (c) The curves show that the local diameter of tube (d_h) from a top-view SEM image depends on the tube x axis.

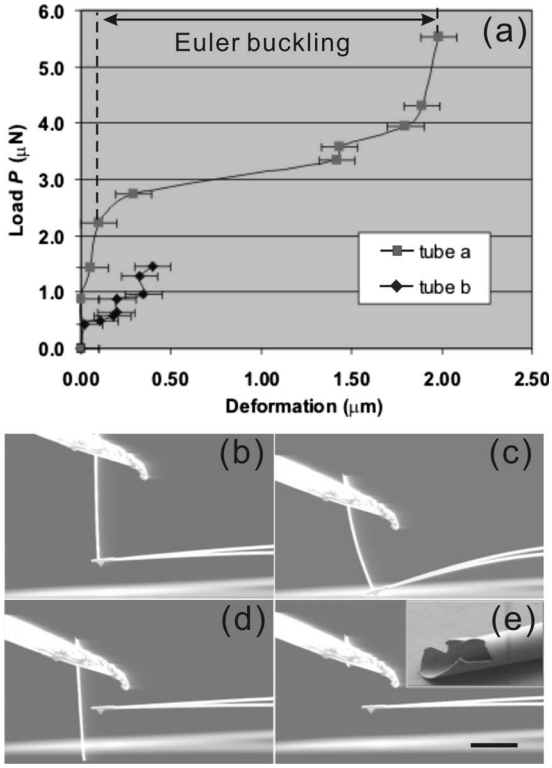

FIG. 4. (a) Experimental curve of force vs displacement resulting from buckling tests for 61.6 and 43.5 μm long SiGe/Si microtubes with 1.6 turn (tube a) and 1.2 turn (tube b), respectively. The Euler buckling regions of the 61.6 μm long tube are marked in the diagram. (b) A tube is stable under axial compressive load. (c) Euler buckling of a 61.6 μm long SiGe/Si tube. (d) The tube recovered from its postbuckling state. (e) The tube was fractured when the load is larger than 5.5 μN. Inset: The fractured region of the SiGe/Si tube.

shape even when bent 180° or more. No catastrophic damage or permanent distortion of their shape was observed in the SEM, indicating that these freestanding microtubes are extremely flexible even under a large deflection. Unlike kinked carbon nanotubes,[6,13] no plastic deformation was found in our tests. The excellent elasticity of these microtubes also implies that the as-grown SiGe/Si heterostructure has a good quality, i.e., nearly free from dislocations. However, with a very large deflection, stress will concentrate quickly at the buckled position of the tube. Eventually, the tube will fracture due to the severe deformation at the buckled position after repeating this bending test. With large deflection angles, i.e., larger than 120°, the tube has a fatigue failure within ten bending test cycles. We have never observed the failure of microtubes by repeated bending tests when the bending angle is smaller than 10°.

According to axial compressive load tests, the dependence of deformation on applied force for SiGe/Si tubes with 1.2 and 1.6 turn is shown in Fig. 4(a). The deformation of the tube is measured as the shortened length of the tube between its fixed end on the manipulator probe and its free end on the AFM cantilever. Distance is measured from the SEM image. For tube a, three deformation regimes can be identified in the buckling test. Initially, the load increases linearly with very small displacement; the tube is in a stable equilibrium state and remains straight [see Fig. 4(b)]. In the second regime the curve becomes flat. The sudden drop of the slope indicates that the tube begins to buckle. Finally, in the third regime, the slope again becomes steep while the

wall of the tube severely bends which is shown in Fig. 4(c). A further increase in load leads to severe local deformation of the tube and, finally, to mechanical fracture of the microtube.

The kink in the curve between the first and the second regime represents a neutral equilibrium of the microtube. The corresponding load is defined as the critical load (P_{cr}). As shown in Fig. 4(a), the value of the critical load of approximately 2.2 μN is determined for a 61.6 μm long, 1.6-turn SiGe/Si microtube. The critical stress (δ_{cr}) can be expressed by $\delta_{cr}=P_{cr}/A$, where A is the cross sectional area of the tube. The critical stress in this tube is 18.4 MPa. In contrast to 1.6-turn microtubes, 1.2-turn tubes (tube b) show less critical load, i.e., 1.5 μN. It should be noted that bilayers scrolled into open "tubes," e.g., 3/4 of a turn, showed a critical stress approximately one order of magnitude smaller than that of the films scrolled by 1.6 turns.

According to Euler's formula,[14] the critical load can be expressed as $P_{cr}=\pi^2 EI/(L_{eff})^2$ in which EI is the flexural rigidity and L_{eff} is the effective length of the tube ($L_{eff}=2L$, for a hinged-fixed boundary condition).[15] Using this formula the calculated critical load for an ideal seamless Si microtube with 61.6 μm length under a hinged-fixed condition is approximately 1.23 μN. The Young's modulus of Si from bulk material,[16] the Si tube with a diameter of 1.25 μm, and a wall width of 19 nm have been assumed. The 1.6-turn rolled-up tube is approximated as a combination of an ideal tube and a 0.6-turn tube, so the cross sectional area is the sum of a thin circular ring and a thin circular arc. For this 1.6-turned ideal tube the critical load is calculated to be 2.0 μN, close to the experimental value (2.2 μN). This result indicates that the mechanical stability of a scrolled microtube with 1.6-turn is very similar to a seamless tube. Whereas the calculated critical load of the 1.2-turn microtube is 3.0 μN, double the experimental value. Based on the above results, it is assumed that the seamless model for calculation of the critical load and the flexural rigidity (EI) of the scrolled microtube is even more accurate for a tightly scrolled tube with the number of turns larger than 1.6, since the cross sectional area shape of rolled-up tube will be even more similar to an ideal seamless ring.[9]

The deviation of the real flexural rigidity of a scrolled microtube and the calculated value from the ideal tube model may result from the difference in the moment of inertia of cross sectional area I. For an ideal seamless tube, I is calculated as $\pi d^3 t/8$ when $t \ll d$,[15] where d and t are the diameter and the wall thickness of the tube, respectively. However, the 1.6-turn rolled-up microtube actually has a seam along the tube axis.

In the rolled-up bilayer, the two edges of the rolled sheet do not bond to form a seamless tube. However, when these edges overlap sufficiently the tube becomes very stable. Surprisingly, the microtubes do not open along the seam when the axial compressive force is larger than the critical load. In addition, the microtubes exhibit an excellent ability to recover from the postbuckling stage to their initial straight shape, as shown in Fig. 4(c). Moreover, in cycling the experiment the critical load remained unchanged after the microtube recovered from the buckled state. This implies that the microtube is elastically deformed and no permanent damage occurs in the SiGe/Si crystalline structure, even after it experiences an unstable state. An interesting observation is that in the third regime, the microtube becomes stiffer again [see Fig. 4(a)]. This may be attributed to the increase in the moment of inertia of the cross sectional area of the microtube. When the microtube is heavily buckled, the neighboring walls of the spiral-like cross section of the tube may interact with each other, leading to a reinforcement of the stiffness of the tube. In addition, glue on the sticky probe may absorb strain energy with a large compressive load, so the load of tube may be overestimated. When the microtube is going to be fractured, the internal (compression) side wall of the tube is open locally, which leads to highly localized stress. In our experiments, this indicated the forthcoming failure of the tube. Figure 4(e) inset shows such a fractured microtube resulting from the axial compression test, in which the curvature of the tube at the local region did not change. FESEM inspections also show that cracked edges prefer to propagate along the cleavage directions, i.e., $\langle 110 \rangle$ and $\langle -110 \rangle$. Thus, the tubes are destroyed in a brittle failure mode, which implies that the SiGe/Si microtubes may have much lower resistance fracture under tension or shear.[15]

Both local buckling and Euler buckling phenomena have been experimentally observed in SiGe/Si microtubes when they are subjected to bending or axial compressive load, respectively. The flexural rigidity of the scrolled SiGe/Si microtube is close to the ideal seamless tube. The self-scrolled SiGe/Si microtubes show no plastic deformation and excellent elastic recovery from a postbuckling state.

The samples were prepared at the Paul Scherrer Institute. The authors thank Dr. J. Gobrecht and Dr. D. Gruetzmacher. They also thank E. Deckardt and A. Weber for their technical support. This work was partially supported by Swiss National Science Foundation (SNSF).

[1] V. Y. Prinz, V. A. Seleznev, A. K. Gutakovsky, A. V. Chehovskiy, V. V. Preobrazhenskii, M. A. Putyato, and T. A. Gavrilova, Physica E (Amsterdam) **6**, 828 (2000).
[2] O. G. Schmidt and K. Eberl, Nature (London) **410**, 168 (2001).
[3] R. Songmuang, C. Deneke, and O. G. Schmidt, Appl. Phys. Lett. **89**, 223109 (2006).
[4] R. Songmuang, A. Rastelli, S. Mendach, and O. G. Schmidt, Appl. Phys. Lett. **90**, 091905 (2007).
[5] O. G. Schmidt and N. Y. Jin-Phillipp, Appl. Phys. Lett. **78**, 3310 (2001).
[6] L. X. Dong, F. Arai, and T. Fukuda, IEEE/ASME Trans. Mechatron. **9**, 350 (2004).
[7] S. V. Golod, V. Y. Prinz, P. Wagli, L. Zhang, O. Kirfel, E. Deckhardt, F. Glaus, C. David, and D. Grutzmacher, Appl. Phys. Lett. **84**, 3391 (2004).
[8] L. Zhang, S. V. Golod, E. Deckardt, V. Prinz, and D. Grutzmacher, Physica E (Amsterdam) **23**, 280 (2004).
[9] L. Zhang, L. X. Dong, and B. J. Nelson, Appl. Phys. Lett. **92**, 143110 (2008).
[10] M. Grundmann, Appl. Phys. Lett. **83**, 2444 (2003).
[11] C. R. Calladine, *Theory of Shell Structures*, 1st ed. (Cambridge University Press, Cambridge, 1983).
[12] G. T. Ju and S. Kyriakides, Int. J. Solids Struct. **29**, 1143 (1992).
[13] M. R. Falvo, G. J. Clary, R. M. Taylor, V. Chi, F. P. Brooks, S. Washburn, and R. Superfine, Nature (London) **389**, 582 (1997).
[14] Stephen P. Timoshenko and James M. Gere, *Theory of Elastic Stability* (McGraw-Hill, New York, 1985).
[15] J. M. Gere, *Mechanics of Materials*, 6th ed. (Brook/Cole-Thomson Learning, Belmont, CA, 2004).
[16] J. J. Wortman and R. A. Evans, J. Appl. Phys. **36**, 153 (1965).